Send Orders for Reprints to reprints@benthamscience.net

Current Chemical Biology, XXXX, *XX*, XX-XX

RESEARCH ARTICLE

Freshwater Bivalve *Coelatura aegyptiaca* as a Sensitive Bioindicator for Zinc Oxide/ Chitosan Nanocomposites Toxicity

Mennatallah H. Abdelaziz[1], Muhammed S. ElRakabawi[2], Ahmed Mohamed Soliman[1] and Ayman Saber Mohamed[1,*]

[1]*Department of Zoology, Faculty of Science, Cairo University 12613, Giza, Egypt;* [2]*Faculty of Biotechnology, October University for Modern Sciences and Arts (MSA), October, Egypt*

ARTICLE HISTORY

Received: September 25, 2024
Revised: January 15, 2025
Accepted: January 16, 2025

DOI:
10.2174/0122127968350685250325165915

Abstract: ***Background*:** Freshwater bivalves are considered effective biomarkers for pollution in aquatic ecosystems. Despite advances in the use of zinc oxide nanoproducts in several sectors, such as food, industry, and medicine, paying attention to their environmental impacts is crucial. The objective of the study was to investigate the mechanisms of zinc oxide-chitosan nanocomposites (ZnO-CS NCs) ecotoxic in freshwater environments using freshwater bivalves Coelatora aegyptica as a sensitive indicator.

***Methods*:** After preparing and characterizing ZnO NPs and ZnO-CS NCs with transmission electron microscopy, ultraviolet spectroscopy, and X-ray diffraction, we exposed the bivalve to three different doses of ZnO NPs and ZnO-CS NCs (12.5, 25, and 50 mg/L) for 7 days.

***Results*:** ZnO-CS NCs concentrations significantly increased malondialdehyde and nitric oxide levels, whereas glutathione and catalase levels decreased in investigated organs. Furthermore, histological changes were detected in the tissues of the gills and mantle.

***Discussion*:** The bivalve organs had varying quantities of MDA, NO, GSH, and CAT. This could be related to the accumulation pattern of heavy metals in each organ, their close interaction with water, or the removal rates.

***Conclusion*:** We concluded from our findings that the toxicity of ZnO-CS NCs on freshwater bivalves causes histological alterations and an oxidative stress response. Moreover, *Coelatura aegyptiaca* was proposed as a highly sensitive bioindicator to monitor water contamination induced by diverse nanoparticles because it can accumulate and concentrate most pollutants, even at low concentrations. As a result, we recommend conducting additional studies with fresh bivalves to evaluate the aquatic ecosystem well and reduce water contamination at both local and worldwide levels.

Keywords: Coelatora aegyptiaca, nanoparticles, chitosan, zinc oxide, oxidative stress, ecotoxicity.

1. INTRODUCTION

Nanocomposites (NCs), one of the early generations in nanotechnology, are formed by combining hetero- or homo-nanoparticle structures for various uses. The combination effect enhances the characteristics of individual nanoparticles in the composite and provides novel functions [1]. The increased production and utilization of nanoparticles in consumer products and industry, along with an extensive number of applications associated with these nanomaterials, have raised apprehensions regarding the possible environmental effect of nanoparticles in various habitats and the detrimental impact on the wellness of people [2-5]. The high surface-to-volume ratio of nanoparticles causes them to have distinct chemical and physical characteristics different from other bulky materials and elevated reactivity potential [4-6].

Furthermore, the formation, characterization, and application of metal-oxide crystals in current electrical and optical devices remains an interesting area for theoretical and experimental research [7]. The antibacterial properties of metal oxides garner interest as an innovative strategy for developing strategies that can substitute organic compounds [8]. The nanoparticle structure, solubility, and interaction modalities with biological systems are emphasized as key aspects in evaluating metal oxide nanoparticle risk [9, 10].

Chitosan nanoparticles (CSNPs) are highly promising polymers and bio-based nanoparticles that have gained significant interest over the past few decades. Their high potential as nanocarriers depends on their ability to encapsulate molecules, such as medications or active substances, transport them to a targeted site, and ensure regulated release [11]. After cellulose, chitosan is the world's second most common natural biopolymer and can be observed in crustacean exoskeletons, molluscan organs, fungi, insects, and yeasts [12]. Furthermore, chitosan is a naturally formed material that finds extensive use in several industries, such

*Address correspondence to this author at the Zoology Department, Faculty of Science, Cairo University 12613, Giza, Egypt;
E-mail: ayman81125@cu.edu.eg

2212-7968/XX $65.00+.00

as food, textiles, farming, water treatment cosmetics, pharmaceutical products, and many other fields [13].

As a result of the appearance of nanotechnology, nano-engineered ZnO has achieved widespread commercial in various product categories due to its excellent transparency and refractive index characteristics. Approximately 550 tons of nano-formulated ZnO are produced annually worldwide [14]. There is growing concern about the potential harm that nano-ZnO could cause to people's health. The nanoparticle toxicity studies were implemented in various biological systems, including human beings, cell-line systems, and animal models, such as rats, zebrafish, and catfish [15, 16]. The nanoparticles can enter living organisms, causing cellular dysfunction by penetrating biological barriers such as cell membranes. The structural and physicochemical characteristics of ZnO nanoparticles induce considerable alterations in biological function. They share in producing reactive oxygen species and stimulating different pathways for signal transduction in particular cells [17]. Consumer and industrial products, such as zinc oxide nanoparticles (ZnO-NP), have raised concerns about their possible ecotoxicological effects if released into the environment. Cellular nanomaterial entry can occur *via* endocytosis, making bivalve mollusks susceptible to nanoparticle toxicity [18].

These days, the scarcity of fresh water has generated widespread concern [19]. Utilizing aquatic invertebrate animal models will be essential in advancing nanoecotoxicology [17]. Freshwater mollusks are a unique species for nanoparticles. Bivalves are filter-feeding and immobile creatures capable of accumulating and concentrating a wide range of contaminants, even at low levels [20]. The Egyptian freshwater bivalves *Caelatura aegyptiaca* are molluscan bivalves that inhabit the Nile River from Assiut to Damietta [21]. For the first time, the current study aimed to use a freshwater bivalve as a sensitive bioindicator for ZnO-CS nanocomposites in the freshwater habitat.

2. MATERIAL AND METHODS

2.1. Materials and Reagents

Chitosan, low molecular weight (75-85% deacetylated), sodium hydroxide (NaOH) (≥98.0-100.5%), and zinc acetate (99.99%) were purchased from Sigma-Aldrich (US).

2.2. Preparing Zinc Oxide Nanoparticles (ZnO NPs)

In solution A, 3.73 mmol of zinc acetate dihydrate was dissolved in 40 ml of ethanol, stirring at 60oC. In solution B, 7.22 mmol of NaOH was dissolved in 320 µL of bi-distilled water and 25 mL of ethanol. After two hours of vigorous and continuous stirring at 60°C, solution B was introduced dropwise to solution A. The mixture was permitted to reach room temperature. Following that, ZnO samples were centrifuged and thoroughly cleaned with new, pure ethanol 3 times. ZnO NPs needed two hours to dry at 60 ^{o}C [22].

2.3. Preparing of Zinc Oxide-Chitosan Nanocomposites (ZnO-CS NCs)

According to [21], the following steps were used to prepare ZnO-CS nanoparticles: A small amount (0.1–1 gm) of ZnO powder was mixed with 100 mL of 1% acetic acid and changed into zinc cations. Then, 1gm of chitosan was added to this mixture and sonicated for 30 min. After magnetic stirring, 1M NaOH was added drop by drop until the pH of the solution reached 10. The mixture was put in a water bath at 40-80 °C for about three hours. After that, the solution was filtered, and the precipitate was washed several times with distilled water. Finally, it was dried in an oven at 50°C for one hour.

2.4. Characterization of ZnO NPs and ZnO-CS NCs

2.4.1. Transmission Electron Microscope Analysis (TEM)

The morphology of ZnONPs and ZnO-CS NCs was imaged using TEM (A JEOL JEM-2100).

2.4.2. Ultraviolet-visible (UV–Vis) Spectral Analysis

To determine the spectroscopic properties of ZnONPs and ZnO-CS NCs, their aqueous solutions were prepared and analyzed using a UV-visible spectrometer (Shimadzu UV-1601). The spectrophotometer worked at 10 nm intervals in the 200–700 nm wavelength range.

2.4.3. X-ray Diffraction (XRD) Analysis

An X-ray diffractometer was used to obtain the structural characteristics of the particles (XRD-6000, Shimadzu, Japan). The device was working at 30 mA and 40 kV and was equipped with a Cu Kα radiation source and Ni filter (wavelength $\lambda = 0.15406$ nm).

2.5. Ethical Consideration

The Institutional Animal Care and Use Committee (IACUC) at the October University for Modern Sciences and Arts, Faculty of Biotechnology, approved the study's methodologies and procedures (MSA2230).

2.6. Experimental Animals

Coelatura aegyptiaca species (6.5–8.5 cm shell wide and 11–14 cm long) was found in the Nile River in the Abu Rawash area of Giza Governorate, Egypt. As soon as we got the samples to the lab, we put them in a glass-reinforced plastic (FRP) case and left them at room temperature. The animals were fed commercial phytoplankton during the whole trial.

2.7. Experimental Design

The current study used the ZnO NPS and ZnO-CS NCs concentrations equal to 12.5, 25, and 50 mg/L. The samples were mixed in water without chlorine for 20 minutes. Five animals per concentration level were exposed for 7 days to ZnO NPS and ZnO-CS NCs. In dechlorinated freshwater, a control group of Bivalves was preserved.

2.8. Determination of ZnO NPs Concentration

ZnO concentrations were measured at 213.856 nm using ICP-OES equipment (ICAP 6500 Duo, Thermo Scientific, Cambridge, UK). Sonication was performed for 20 minutes before the measurement. The tests were run three times.

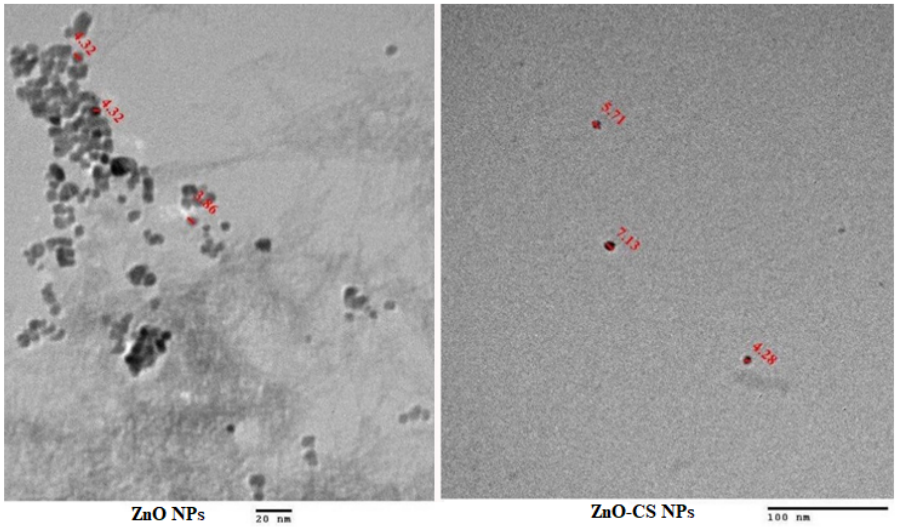

Fig. (1). TEM analysis of zinc oxide NPs and zinc oxide-chitosan NCs. (*A higher resolution / colour version of this figure is available in the electronic copy of the article*).

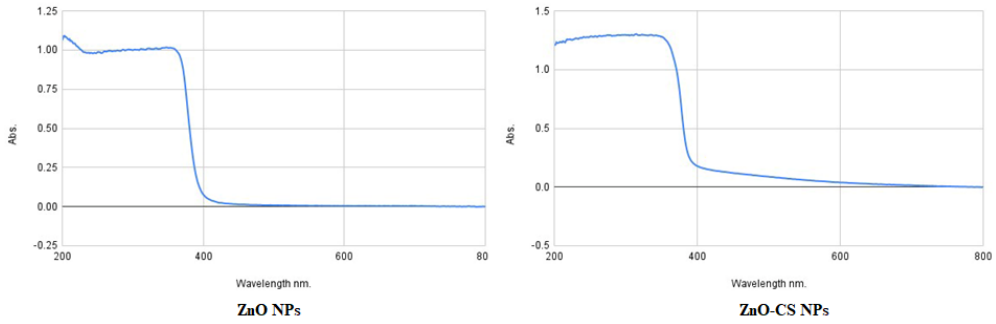

Fig. (2). UV-vis absorption spectrum analysis of zinc oxide NPs and zinc oxide-chitosan NCs. (*A higher resolution / colour version of this figure is available in the electronic copy of the article*).

2.9. Preparation of Samples

Once carefully removed, the soft parts, including the mantle, foot, digestive gland, and gills, were rinsed with 0.9 percent ice-cold saline. Tissues were mixed with a 10% w/v phosphate buffer (pH 7.4) warmed to room temperature. The homogenate was centrifuged at 3000 rpm and 4°C for 15 min to prepare it for biochemical examination [23, 24].

2.10. Evaluation of Oxidative Stress

Oxidative stress biomarkers were measured using the supernatant of the tissue homogenate to determine lipid peroxidation, which was measured by the formation of malondialdehyde (MDA) [25], catalase (CAT), glutathione (GSH) [26], and nitric oxide (NO) [27].

2.11. Histopathological Examination

Following dissection, the tissues of the gills and mantle were preserved in a 10% neutral-buffered formalin. The conserved specimens undergo washing, dehydration, and embedding in paraffin wax at temperatures ranging from 58 to 60 °C. Paraffin cubes were cut to appropriate sizes, and tissues were sectioned using a microtome with a thickness of five µm. After removing the paraffin, the slides were rehydrated and stained with hematoxylin and eosin.

2.12. Statistical Study

Values were reported as means ± SE. SPSS 25.0 for Windows was used for statistical analysis. One-way ANOVA with Duncan post hoc test was used to compare group means. Statistical significance occurs with $p < 0.05$.

3. RESULTS

3.1. ZnO and ZnO-Chitosan Nanoparticles Characterization

The TEM micrographs revealed the roughly homogenous spherical shape of the ZnO NPs and ZnO-CS NPs with average diameters of 4 nm for ZnO NPs and 4-7 nm for ZnO-CS NPs (Fig. **1**).

UV-visible spectroscopy is a very straightforward and sensitive method for detecting the formation of metallic and metal oxide nanoparticles. UV spectra of ZnO-CS nanoparticles showed that it had λ max at 348, 322 nm, like those of ZnO NPs, which exhibited a maximum at 315, 263 nm (Fig. **2**).

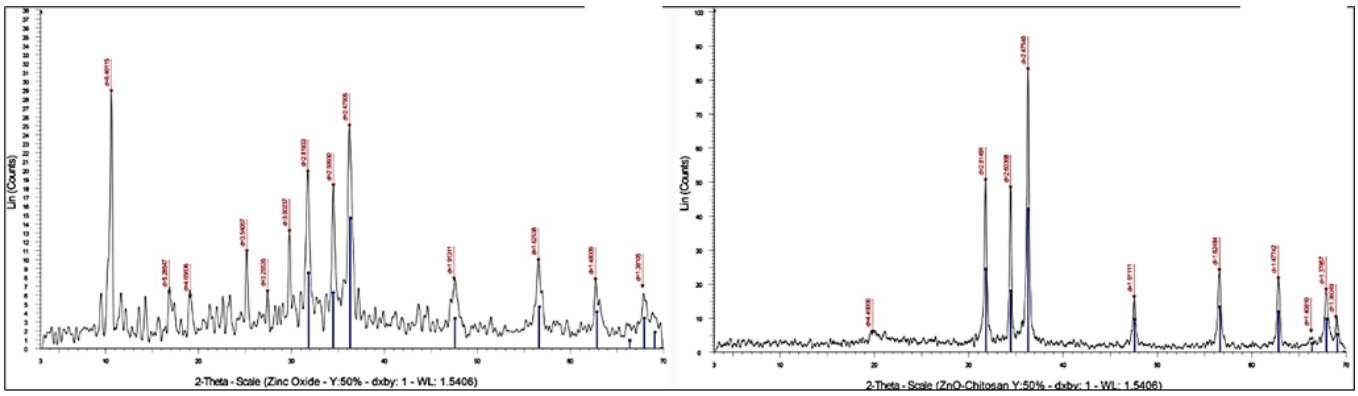

Fig. (3). X-ray diffraction analysis of zinc oxide NPs and zinc oxide-chitosan NCs. (*A higher resolution / colour version of this figure is available in the electronic copy of the article*).

X-ray diffraction evaluation identified the crystalline shape of the prepared ZnO and ZnO-CS nanoparticles. The patterns demonstrated that the ZnO-CS nanoparticles were well-crystallized. ZnO and ZnO-CS NPs had distinct XRD peaks at 2θ values of Peaks at 2θ=32.35°, 33.89°, 36.81°, 37.94°, 39.99°, and 44.42° correspond to the crystal planes of (1 0 0), (0 0 2), (1 0 1), (1 1 0), (1 0 3), and (1 1 2) hexagonal zinc oxide (Fig. **3**). The diffraction peaks were all consistent with the hexagonal wurtzite structure of ZnO (JCPDS card 36-1451) [28] Using the Debye Scherrer formula, the average size of ZnO NPs was calculated to be 98 nm and ZnO-CS 45 nm, indicating that the inclusion of chitosan as a stabilizer lowered the agglomeration rate in the synthesis of ZnO NPs, hence reducing the crystallite size of nanoparticles.

All peaks of XRD spectra were compared with the standard peaks in JCPDS files, resulting in excellent matching of all samples.

3.2. ZnO NPs Concentration

The levels of zinc oxide in the zinc oxide-Chitosan nanocomposite solutions were found to be 9, 20, and 42 mg/L for each exposed concentration of 12.5, 25, and 50 mg/L, respectively.

3.3. Impact of ZnO and ZnO-Chitosan NPs on Organ Oxidative State in *Coelatura aegyptiaca*

3.3.1. Malondialdehyde (MDA) and Nitric Oxide (NO)

MDA assay revealed a statistically significant increase (p<0.05) in concentration between all treated and the control groups, except for the lowest dose of ZnO NPs in the mantle. There was a significant change (p<0.05) in MDA concentration between ZnO nanoparticles compared to ZnO-CS nanoparticles in most tissues, as shown in (Table **1**).

NO assay showed a significant increase (p<0.05) in concentration between all treated and the control groups, except for the lowest dose of ZnO NPs in the mantle and foot. Also, there was a significant increase (p<0.05) in NO concentration between ZnO and ZnO-CS nanoparticles across all organs (Table **2**).

3.3.2. Glutathione (GSH) and Catalase (CAT)

Assays of the GSH levels showed a significant reduction (p<0.05) between the control and all treated groups. Likewise, there was a significant decrease (p<0.05) in GSH concentration between ZnO and ZnO-CS nanoparticles across all organs at the lowest dose. Still, there was no significant change between ZnO and ZnO-CS at 25 and 50 mg doses in mantle, as evident in Table (**3**).

CAT assay indicated a significant decrease (p<0.05) in all organs between the control and treated groups. Likewise, there was a significant decrease (p<0.05) in CAT concentration between ZnO and ZnO-CS nanoparticles, as shown in Table (**4**) across all organs, except for the highest dose in the mantle.

3.4. Histological Examination of the Gills

The control animal gills revealed the typical bivalve ctenidium structure, including filaments and water channels. Each gill filament contained two chitinous rods, a central tissue core, and well-organized epithelial cells with lateral and frontal cilia. (Fig. **4**). However, the lateral and frontal cilia had shed off after being subjected to ZnO NPs and ZnO-CS NCs for 7 days, and the gill filament lumen housed blood cells. The gill filaments were also severely disordered, and the expansion of the gill lumen caused cellular damage.

3.5. Histopathology of the Mantle

A plicated integument (PI), which represents the epithelial layer, and a connective tissue layer with granulocytes (GC) were seen in the mantle's light micrograph. A layer of somatic musculature (SM) was also discovered in healthy tissue. The plicated integument comprised mucous and ciliated columnar epithelial cells (CEC). The muscular layer of the mantle, on the other hand, has longitudinal cross-sections of myocytes (Fig. **5**). Massive degeneration in the mantle, such as muscle bundle breakage, muscular atrophy, and granulocyte expansion, were seen after brought to ZnO NPs and ZnO-CS NCs. Although both chemicals were present, the ZnO-CS NCs tissues showed a more pronounced impact.

Table 1. Effect zinc oxide nanoparticles (ZnO NPs) and ZnO-Chitosan nanoparticles (ZnO-CS NCs) on MDA (nM/g.tissue) in four different organs of *Coelatura aegyptiaca*.

Groups	Concentrations (mg/L)	Organ			
		Digestive Gland	Gills	Mantle	Foot
Control	0	1.20 ± 0.05^{a}	0.94 ± 0.08^{a}	0.64 ± 0.07^{a}	0.88 ± 0.04^{a}
ZnO NPs	12.5	3.16 ± 0.22^{b}	1.16 ± 0.02^{b}	0.61 ± 0.03^{a}	1.13 ± 0.03^{b}
	25	3.64 ± 0.02^{cd}	1.31 ± 0.03^{c}	0.86 ± 0.02^{bc}	1.45 ± 0.02^{c}
	50	3.82 ± 0.02^{d}	1.68 ± 0.02^{d}	1.23 ± 0.19^{d}	1.81 ± 0.01^{d}
ZnO-CS NCs	12.5	3.46 ± 0.18^{bc}	1.36 ± 0.03^{c}	0.71 ± 0.05^{bc}	1.61 ± 0.03^{e}
	25	3.93 ± 0.05^{d}	1.64 ± 0.02^{d}	0.92 ± 0.03^{c}	2.12 ± 0.04^{f}
	50	4.43 ± 0.04^{e}	1.87 ± 0.01^{e}	1.25 ± 0.04^{d}	2.56 ± 0.06^{g}

Note: Values presented as means ± standard error ($n = 5$). Values that do not share common superscript letter are considered significantly different ($P < 0.05$).

Table 2. Effect zinc oxide nanoparticles (ZnO NPs) and ZnO-Chitosan nanoparticles (ZnO-CS NCs) on NO (µM/g.tissue) in four different organs of *Coelatura aegyptiaca*.

Groups	Concentrations (mg/L)	Organ			
		Digestive Gland	Gills	Mantle	Foot
Control	0	5.04 ± 0.67^{a}	6.05 ± 0.25^{a}	6.67 ± 0.93^{a}	9.46 ± 0.88^{a}
ZnO NPs	12.5	9.46 ± 0.44^{b}	10.07 ± 0.84^{b}	7.09 ± 0.38^{a}	11.41 ± 0.83^{a}
	25	14.70 ± 0.91^{c}	11.60 ± 1.40^{b}	9.10 ± 0.44^{ab}	17.19 ± 0.85^{b}
	50	18.98 ± 0.94^{d}	19.19 ± 1.00^{c}	17.51 ± 1.34^{c}	25.63 ± 0.86^{d}
ZnO-CS NCs	12.5	19.26 ± 0.62^{d}	17.68 ± 0.77^{c}	11.43 ± 0.80^{b}	19.58 ± 0.47^{c}
	25	39.14 ± 2.47^{e}	22.95 ± 0.47^{d}	16.40 ± 1.02^{cd}	27.50 ± 0.27^{d}
	50	46.13 ± 1.80^{f}	29.22 ± 0.50^{e}	19.44 ± 0.46^{d}	37.03 ± 1.20^{e}

Note: Values presented as means ± standard error ($n = 5$). Values that do not share common superscript letter are considered significantly different ($P < 0.05$).

Table 3. Effect zinc oxide nanoparticles (ZnO NPs) and ZnO-Chitosan nanoparticles (ZnO-CS NCs) on GSH (mM/g.tissue) in four different organs of *Coelatura aegyptiaca*.

Groups	Concentrations (mg/L)	Organ			
		Digestive Gland	Gills	Mantle	Foot
Control	0	2.87 ± 0.06^{f}	3.99 ± 0.16^{e}	3.54 ± 0.05^{e}	2.85 ± 0.10^{g}
ZnO NPs	12.5	2.56 ± 0.03^{e}	3.61 ± 0.04^{d}	3.07 ± 0.07^{d}	2.30 ± 0.05^{f}
	25	2.19 ± 0.04^{d}	3.12 ± 0.10^{c}	2.59 ± 0.08^{b}	2.01 ± 0.06^{e}
	50	2.02 ± 0.06^{cd}	2.68 ± 0.03^{b}	2.20 ± 0.05^{a}	1.69 ± 0.01^{d}
ZnO-CS NCs	12.5	1.89 ± 0.06^{cd}	3.43 ± 0.13^{d}	2.81 ± 0.02^{c}	1.01 ± 0.03^{c}
	25	1.20 ± 0.05^{b}	2.92 ± 0.10^{bc}	2.45 ± 0.03^{b}	0.69 ± 0.01^{b}
	50	0.95 ± 0.04^{a}	2.36 ± 0.07^{a}	2.23 ± 0.03^{a}	0.30 ± 0.07^{a}

Note: Values presented as means ± standard error ($n = 5$). Values that do not share common superscript letter are considered significantly different ($P < 0.05$).

Table 4. Effect zinc oxide nanoparticles (ZnO NPs) and ZnO-Chitosan nanoparticles (ZnO-CS NCs) on CAT (U/g.tissue) in four different organs of *Coelatura aegyptiaca*.

Groups	Concentrations (mg/L)	Organ			
		Digestive Gland	Gills	Mantle	Foot
Control	0	15.84 ± 0.41^{f}	21.32 ± 0.49^{e}	18.60 ± 0.39^{e}	14.05 ± 0.54^{f}
ZnO NPs	12.5	10.26 ± 0.29^{e}	12.26 ± 0.43^{d}	11.00 ± 0.35^{d}	9.33 ± 0.19^{d}
	25	8.82 ± 0.22^{d}	7.36 ± 0.13^{c}	8.33 ± 0.25^{c}	6.26 ± 0.19^{b}
	50	5.33 ± 0.13^{cd}	5.44 ± 0.28^{b}	4.48 ± 0.11^{a}	4.50 ± 0.19^{a}
ZnO-CS NCs	12.5	5.98 ± 0.18^{cd}	5.80 ± 0.26^{b}	8.48 ± 0.11^{c}	8.95 ± 0.19^{d}
	25	4.37 ± 0.11^{b}	4.38 ± 0.06^{a}	5.47 ± 0.06^{b}	7.97 ± 0.23^{c}
	50	1.71 ± 0.06^{a}	3.80 ± 0.04^{a}	4.47 ± 0.06^{a}	4.22 ± 0.23^{e}

Note: Values presented as means ± standard error ($n = 5$). Values that do not share common superscript letter are considered significantly different ($P < 0.05$).

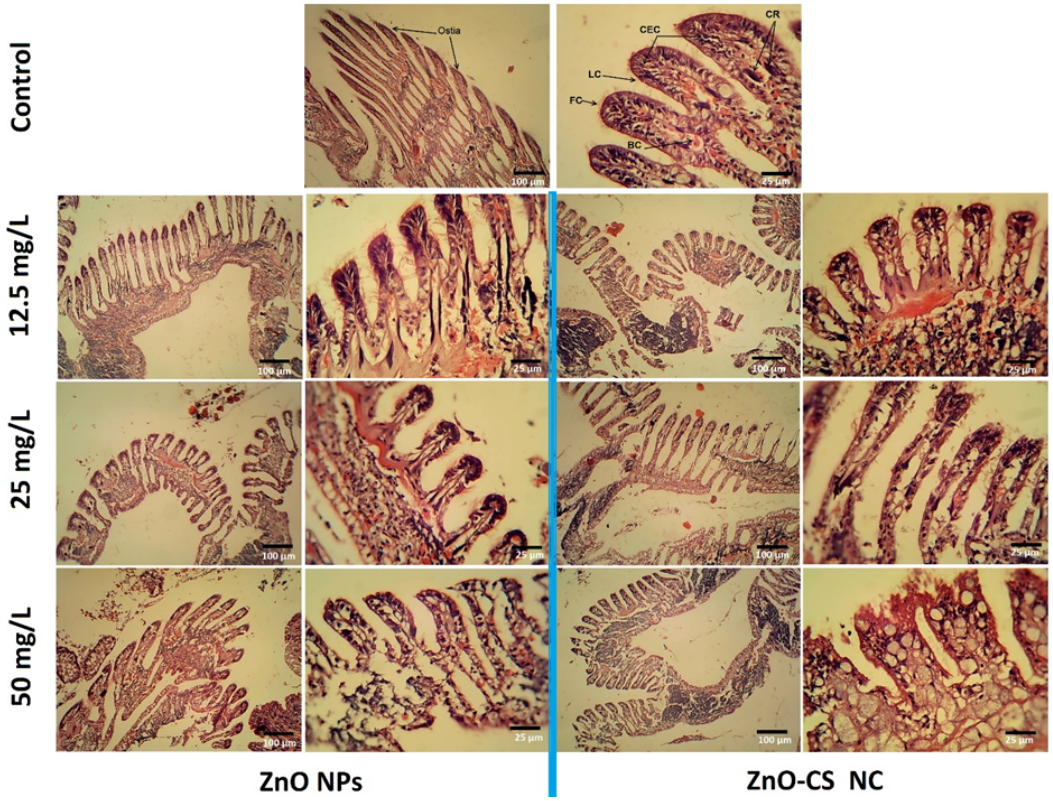

Fig. (4). Histological sections (H&E) of Coelatura aegyptiaca' gills exposed to ZnO NPs and ZnO-CS NCs. CR: chitinous rods, BC: blood cells, CEC: ciliated columnar epithelial cells, FC: frontal cilia, and LC: lateral cilia. (*A higher resolution / colour version of this figure is available in the electronic copy of the article*).

4. DISCUSSION

Heavy metal leakage into aquatic ecosystems is highly hazardous to the ecosystem due to its toxic properties [29-31]. Water pollution is a critical issue with serious consequences for human health, wildlife health, and the aquatic ecosystem. One of the most dangerous hazards is Water contamination from industry nanotechnologies and its by-products [32]. Previous studies have shown that Zn is hazardous to aquatic organisms at sublethal concentrations ranging from 0.8 to 100 mg/L [33, 34].

Oxidative stress (OXS) is an adequate factor that was proposed as one of the possible causes for the toxicity of ZnO-CS NCs in *Caelatura aegyptiaca* freshwater bivalves since cells respond to OXS by exhibiting several defensive mechanisms that may be directly assessed to be changes in biochemical or genomic expression [35]. ROS production

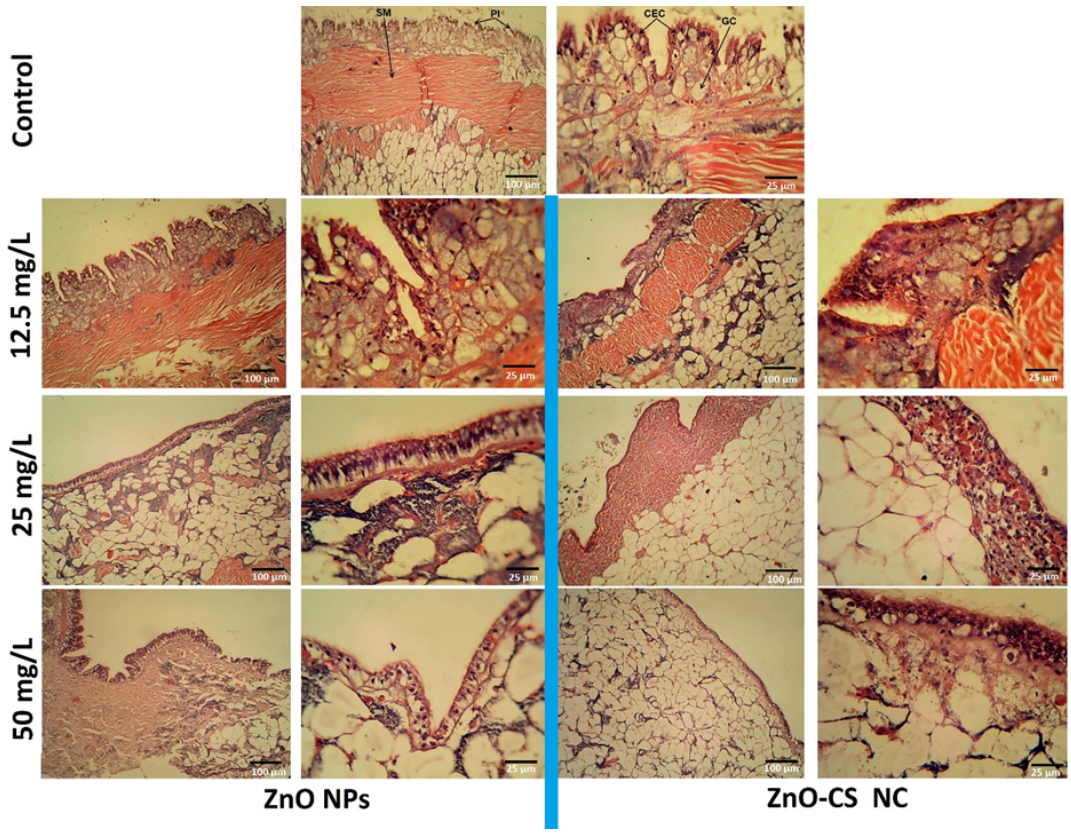

Fig. (5). Histological sections (H&E) of Coelatura aegyptiaca's mantle exposed to ZnO NPs and ZnO-CS NCs. GC: granulocytes, CEC: ciliated columnar epithelial cells, SM: somatic musculature, and PI: plicated integument. (*A higher resolution / colour version of this figure is available in the electronic copy of the article*).

and cellular OXS were earlier proposed as potential NP toxicity mechanisms [36, 37]. The risk of ROS generation is influenced by the extent of stress and the physicochemical conditions within the cell (*i.e.*, antioxidant status and redox state). Stress produces active oxygen, which is known to be harmful and can cause lipid peroxidation and enzyme deactivation [38].

Malondialdehyde (MDA) is a highly reactive metabolic product generated by a series of reactions induced by lipid peroxide and the effect of oxygen-free radicals on tissues [20, 39]. MDA levels were elevated significantly in the ZnO NPs and ZnO-CS NCs groups compared to the control groups. According to [40], increased MDA levels cause increased lipid peroxidation, resulting in tissue damage, impairing antioxidant defenses, and increased free radical production. The highest ZnO-CS NCs concentration induced a significant elevation in hepatopancreas (Digestive gland) MDA level when compared to the ZnO group, supporting the approach posits that filter-feeding bivalves are a suitable target for NPs in aquatic ecosystems [41].

NO is produced in mollusks by mobile defense cells kno wn as hemocytes. NO synthase (NOS) is an enzyme that catalyzes the oxidation of L-arginine into L-citrulline producing NO molecules [42]. The current study revealed a significant increase in nitric oxide content in the Digestive gland and gills of ZnO NPs treated bivalves compared to control. Furthermore, a significant increase in all evaluated organs of ZnO-CS NCs treated bivalves was found in a concentration-dependent manner compared to ZnO NPs, indicating that ZnO-CS NCs increased NO production to suppress the stress induced by nanoparticle exposure. This investigation corroborated previous findings reported in [43], where it was proposed that NPs cause oxidative burst and NO production in bivalve hemocytes [44].

Reduced glutathione (GSH) is thought to act as an essential cellular protective factor *versus* reactive oxygen metabolites by acting as a substrate for glutathione peroxidase [45]. GSH concentrations declined significantly in ZnO NPs groups compared to the control group. Similarly, there was a significant decrease in GSH concentrations between ZnO and ZnO-CS nanoparticles across all organs at the lowest dose, except for (25 and 50 mg/L) doses in the mantle, which showed no significant change. According to [46], the decrease in GSH content is accompanied by increased lipid peroxidation. Furthermore, mollusks respond to metal exposure by depleting GSH content in the digestive gland [47].

Catalase (CAT) is a critical element in the defensive antioxidant system, which works together to protect against ROS [48]. It catalyzes the reaction that converts hydrogen peroxide to water and oxygen [49]. Antioxidant enzymes, such as peroxidase and catalase, protect cells from oxygen generation's damaging impacts by maintaining relatively low internal reactive oxygen levels and mitigating the damage caused by their high reactions [50]. The study recorded a significant decrease in CAT activity between the control group and ZnO NPs/ ZnO-CS NPs treated groups in all or-

gans. The decline in catalase (CAT) activity could be ascribed to a decrease in the production of proteins, leading to an elevation in the peroxidation end product MDA [51].

The bivalve organs had varying quantities of MDA, NO, GSH, and CAT. This could be related to the accumulation pattern of heavy metals in each organ, their close interaction with water, or the removal rates [52-54].

CONCLUSION

The present study exposed freshwater bivalves to zinc oxide NPs and zinc oxide-chitosan NCs, resulting in oxidative elevation impacts and tissue changes in the investigated organs. *Coelatura aegyptiaca* was revealed to be an effective bioindicator for water pollution by nanoparticle contamination.

AUTHORS' CONTRIBUTION

The authors confirm their contribution to the paper as follows: study conception and design: A.S.M.; data collection: M.S.E.; draft manuscript: M.H.A.; Methodology: A.M.S. All authors reviewed the results and approved the final version of the manuscript.

LIST OF ABBREVIATIONS

CSNPs	=	Chitosan Nanoparticles
NaOH	=	Sodium Hydroxide
NCs	=	Nanocomposites
TEM	=	Transmission Electron Microscope Analysis
ZnO-CS NCs	=	Zinc Oxide-chitosan Nanocomposites
ZnO-NP	=	Zinc Oxide Nanoparticles

ETHICS APPROVAL AND CONSENT TO PARTICIPATE

The Institutional Animal Care and Use Committee (IACUC) at the October University for Modern Sciences and Arts, Faculty of Biotechnology, approved the study's methodologies and procedures (MSA2230).

HUMAN AND ANIMAL RIGHTS

The reported experiments in accordance with the standards set forth in "Guide for the Care and Use of Laboratory Animals." This study adheres to internationally accepted standards for animal research, following the 3Rs principle. The ARRIVE guidelines were employed for reporting experiments involving live animals, promoting ethical research practices.

CONSENT FOR PUBLICATION

Not applicable.

AVAILABILITY OF DATA AND MATERIALS

The authors confirm that the data supporting the findings of this research are available within the article.

FUNDING

None.

CONFLICT OF INTEREST

The authors declare no conflict of interest, financial or otherwise.

ACKNOWLEDGEMENTS

Declared none.

REFERENCES

[1] Giannousi, K.; Menelaou, M.; Arvanitidis, J.; Angelakeris, M.; Pantazaki, A.; Dendrinou-Samara, C. Hetero-nanocomposites of magnetic and antifungal nanoparticles as a platform for magneto-mechanical stress induction in Saccharomyces cerevisiae. *J. Mater. Chem. B Mater. Biol. Med.,* **2015**, *3*(26), 5341-5351. http://dx.doi.org/10.1039/C5TB00734H PMID: 32262610

[2] Simonet, B.M.; Valcárcel, M. Monitoring nanoparticles in the environment. *Anal. Bioanal. Chem.,* **2009**, *393*(1), 17-21. http://dx.doi.org/10.1007/s00216-008-2484-z PMID: 18974979

[3] Salieri, B.; Righi, S.; Pasteris, A.; Olsen, S.I. Freshwater ecotoxicity characterisation factor for metal oxide nanoparticles: A case study on titanium dioxide nanoparticle. *Sci. Total Environ.,* **2015**, *505*, 494-502. http://dx.doi.org/10.1016/j.scitotenv.2014.09.107 PMID: 25461051

[4] Girardello, F.; Custódio Leite, C.; Vianna Villela, I.; da Silva Machado, M.; Luiz Mendes Juchem, A.; Roesch-Ely, M.; Neves Fernandes, A.; Salvador, M.; Antonio Pêgas Henriques, J. Titanium dioxide nanoparticles induce genotoxicity but not mutagenicity in golden mussel Limnoperna fortunei. *Aquat. Toxicol.,* **2016**, *170*, 223-228. http://dx.doi.org/10.1016/j.aquatox.2015.11.030 PMID: 26675368

[5] Girardello, F.; Leite, C.C.; Branco, C.S.; Roesch-Ely, M.; Fernandes, A.N.; Salvador, M.; Henriques, J.A.P. Antioxidant defences and haemocyte internalization in Limnoperna fortunei exposed to TiO2 nanoparticles. *Aquat. Toxicol.,* **2016**, *176*, 190-196. http://dx.doi.org/10.1016/j.aquatox.2016.04.024 PMID: 27152940

[6] Mallevre, F.; Fernandes, T.F.; Aspray, T.J. Silver, zinc oxide and titanium dioxide nanoparticle ecotoxicity to bioluminescent *Pseudomonas putida* in laboratory medium and artificial wastewater. *Environ. Pollut.,* **2014**, *195*, 218-225. http://dx.doi.org/10.1016/j.envpol.2014.09.002 PMID: 25261625

[7] Ramana, C.V.; Carbajal-Franco, G.; Vemuri, R.S.; Troitskaia, I.B.; Gromilov, S.A.; Atuchin, V.V. Optical properties and thermal stability of germanium oxide (GeO2) nanocrystals with α-quartz structure. *Mater. Sci. Eng. B,* **2010**, *174*(1-3), 279-284. http://dx.doi.org/10.1016/j.mseb.2010.03.060

[8] Dyshlyuk, L.; Babich, O.; Ivanova, S.; Vasilchenco, N.; Atuchin, V.; Korolkov, I.; Russakov, D.; Prosekov, A. Antimicrobial potential of ZnO, TiO2 and SiO2 nanoparticles in protecting building materials from biodegradation. *Int. Biodeterior. Biodegradation,* **2020**, *146*, 104821. http://dx.doi.org/10.1016/j.ibiod.2019.104821

[9] Wang, Z.; Lee, Y.H.; Wu, B.; Horst, A.; Kang, Y.; Tang, Y.J.; Chen, D.R. Anti-microbial activities of aerosolized transition metal oxide nanoparticles. *Chemosphere,* **2010**, *80*(5), 525-529. http://dx.doi.org/10.1016/j.chemosphere.2010.04.047 PMID: 20478610

[10] Wu, B.; Wang, Y.; Lee, Y.H.; Horst, A.; Wang, Z.; Chen, D.R.; Sureshkumar, R.; Tang, Y.J. Comparative eco-toxicities of nano-ZnO particles under aquatic and aerosol exposure modes. *Environ. Sci. Technol.,* **2010**, *44*(4), 1484-1489. http://dx.doi.org/10.1021/es9030497 PMID: 20102184

[11] Yanat, M.; Schroën, K. Preparation methods and applications of chitosan nanoparticles; With an outlook toward reinforcement of biodegradable packaging. *React. Funct. Polym.,* **2021**, *161*, 104849. http://dx.doi.org/10.1016/j.reactfunctpolym.2021.104849

[12] Taylor, P.; Tharanathan, R.N.; Kittur, F.S. Critical reviews in food science and nutrition chitin — The undisputed biomolecule of great potential chitin — The undisputed biomolecule of great potential. *Crit. Rev. Food Sci. Nutr.,* **2003**, *43*, 61-87.

[13] Bui, V.; Park, D.; Lee, Y.C. Chitosan combined with ZnO, TiO2 and Ag nanoparticles for antimicrobial wound healing applications: A mini review of the research trends. *Polymers,* **2017**, *9*(1), 21.
http://dx.doi.org/10.3390/polym9010021 PMID: 30970696

[14] Piccinno, F.; Gottschalk, F.; Seeger, S.; Nowack, B. Industrial production quantities and uses of ten engineered nanomaterials in Europe and the world. *J. Nanopart. Res.,* **2012**, *14*(9), 1109.
http://dx.doi.org/10.1007/s11051-012-1109-9

[15] Sharma, V.; Anderson, D.; Dhawan, A. Zinc oxide nanoparticles induce oxidative DNA damage and ROS-triggered mitochondria mediated apoptosis in human liver cells (HepG2). *Apoptosis,* **2012**, *17*(8), 852-870.
http://dx.doi.org/10.1007/s10495-012-0705-6 PMID: 22395444

[16] Lozano, T.; Rey, M.; Rojas, E.; Moya, S.; Fleddermann, J.; Estrela-Lopis, I.; Donath, E.; Wang, B.; Mao, Z.; Gao, C.; González-Fernández, Á. Cytotoxicity effects of metal oxide nanoparticles in human tumor cell lines. *J. Phys. Conf. Ser.,* **2011**, *304*, 012046.
http://dx.doi.org/10.1088/1742-6596/304/1/012046

[17] Fahmy, S.R.; Abdel-Ghaffar, F.; Bakry, F.A.; Sayed, D.A. Ecotoxicological effect of sublethal exposure to zinc oxide nanoparticles on freshwater snail *Biomphalaria alexandrina*. *Arch. Environ. Contam. Toxicol.,* **2014**, *67*(2), 192-202.
http://dx.doi.org/10.1007/s00244-014-0020-z PMID: 24736985

[18] Moloukhia, H.; Sleem, S. Bioaccumulation, fate and toxicity of two heavy metals common in industrial wastes in two aquatic molluscs. *J. Am. Sci.,* **2011**, *7*, 459-464.

[19] Mohamed, A.S.; Bin Dajem, S.; Al-Kahtani, M.; Ali, S.B.; Ibrahim, E.; Morsy, K.; Fahmy, S.R. Silver/chitosan nanocomposites induce physiological and histological changes in freshwater bivalve. *J. Trace Elem. Med. Biol.,* **2021**, *65*, 126719.
http://dx.doi.org/10.1016/j.jtemb.2021.126719 PMID: 33517023

[20] Mohamed, A.S.; Bin Dajem, S.; Al-Kahtani, M.; Ali, S.B.; Alshehri, M.; Shati, A.; Morsy, K.; Fahmy, S.R. Freshwater clam as a potential bioindicator for silver/saponin nanocomposites toxicity. *Bull. Environ. Contam. Toxicol.,* **2020**, *105*(6), 827-834.
http://dx.doi.org/10.1007/s00128-020-03038-x PMID: 33156393

[21] Omar, T.Y.; Elshenawy, H.I.A.; Abdelfattah, M.A.; Al Shawoush, A.M.; Mohamed, A.S.; Saad, D.Y. Biointerfrence between Zinc Oxide/Alginate nanocomposites and freshwater bivalve. *Biointerface Res. Appl. Chem.,* **2022**, *13*(3), 277.
http://dx.doi.org/10.33263/BRIAC133.277

[22] Cao, D.; Gong, S.; Shu, X.; Zhu, D.; Liang, S. Preparation of ZnO nanoparticles with high dispersibility based on oriented attachment (OA) process. *Nanoscale Res. Lett.,* **2019**, *14*(1), 210.
http://dx.doi.org/10.1186/s11671-019-3038-3 PMID: 31222635

[23] Mohamed, A.S.; Elkareem Mustafa, M.A.; Soliman, A.M.; Fahmy, S.R. Potential inhibition of ehrlich ascites carcinoma by naja nubiae crude venom in swiss albino mice. *Biointerface Res. Appl. Chem.,* **2021**, *12*(6), 7741-7751.
http://dx.doi.org/10.33263/BRIAC126.77417751

[24] Yousse, A.; Baiomy, A.; Fahmy, S.R.; Mohamed, A.; Saad, D.; Desoky, R. Potential anti-osteoporotic effect of *Allolobophora caliginosa* extract in orchiectomized rats. *Pharm. Sci. Asia,* **2022**, *49*(2), 138-146.
http://dx.doi.org/10.29090/psa.2022.02.21.144

[25] Mohamed, A.S.; Ibrahim, W.M.; Zaki, N.I.; Ali, S.B.; Soliman, A.M. Effectiveness of *Coelatura aegyptiaca* extract combination with atorvastatin on experimentally induced hyperlipidemia in rats. *Evid. Based Complement. Alternat. Med.,* **2019**, *2019*, 1-9.
http://dx.doi.org/10.1155/2019/9726137 PMID: 30713580

[26] Beutler, E.; Duron, O.; Kelly, B.M. Improved method for the determination of blood glutathione. *J. Lab. Clin. Med.,* **1963**, *61*, 882-888.
PMID: 13967893

[27] Montgomery, H.; Dymock, J.F. Determination of nitrite in water. *Analyst,* **1961**, *86*, 414.

[28] Zaman, H.G.; Baloo, L.; Aziz, F.; Kutty, S.R.; Ashraf, A. COD adsorption and optimization from produced water using chitosan–ZnO nanocomposite. *Appl. Nanosci.,* **2022**, *12*(6), 1885-1898.
http://dx.doi.org/10.1007/s13204-022-02392-y

[29] Gupta, V.K.; Rastogi, A.; Dwivedi, M.K.; Mohan, D. Process Development for the Removal of Zinc and Cadmium from Wastewater Using Slag—A Blast Furnace Waste Material. *Separation Sci. Technol.,* **1997**, *32*(17), 2883-2912.
http://dx.doi.org/10.1080/01496399708002227

[30] Burakov, A.E.; Galunin, E.V.; Burakova, I.V.; Kucherova, A.E.; Agarwal, S.; Tkachev, A.G.; Gupta, V.K. Adsorption of heavy metals on conventional and nanostructured materials for wastewater treatment purposes: A review. *Ecotoxicol. Environ. Saf.,* **2018**, *148*, 702-712.
http://dx.doi.org/10.1016/j.ecoenv.2017.11.034 PMID: 29174989

[31] Atuchin, V.V.; Asyakina, L.K.; Serazetdinova, Y.R.; Frolova, A.S.; Velichkovich, N.S.; Prosekov, A.Y. Microorganisms for bioremediation of soils contaminated with heavy metals. *Microorganisms,* **2023**, *11*(4), 864.
http://dx.doi.org/10.3390/microorganisms11040864 PMID: 37110287

[32] Saravanan, R.; Karthikeyan, N.; Gupta, V.K.; Thirumal, E.; Thangadurai, P.; Narayanan, V.; Stephen, A. ZnO/Ag nanocomposite: An efficient catalyst for degradation studies of textile effluents under visible light. *Mater. Sci. Eng. C,* **2013**, *33*(4), 2235-2244.
http://dx.doi.org/10.1016/j.msec.2013.01.046 PMID: 23498253

[33] Németh, I.; Molnár, S.; Vaszita, E.; Molnár, M. The biolog EcoPlate™ technique for assessing the effect of metal oxide nanoparticles on freshwater microbial communities. *Nanomaterials,* **2021**, *11*(7), 1777.
http://dx.doi.org/10.3390/nano11071777 PMID: 34361164

[34] Sanpradit, P.; Byeon, E.; Lee, J.S.; Peerakietkhajorn, S. Ecotoxicological, ecophysiological, and mechanistic studies on zinc oxide (ZnO) toxicity in freshwater environment. *Comp. Biochem. Physiol. C Toxicol. Pharmacol.,* **2023**, *273*, 109720.
http://dx.doi.org/10.1016/j.cbpc.2023.109720 PMID: 37586582

[35] Kovochich, M.; Xia, T.; Xu, J.; Yeh, J.I. Principles and procedures to assess nanomaterial toxicity. In: *Environmental Nanotechnology: Applications and Impacts of Nanomaterials*; The McGraw-Hill Companies, **2007**; pp. 205-230.

[36] Yang, H.; Liu, C.; Yang, D.; Zhang, H.; Xi, Z. Comparative study of cytotoxicity, oxidative stress and genotoxicity induced by four typical nanomaterials: The role of particle size, shape and composition. *J. Appl. Toxicol.,* **2009**, *29*(1), 69-78.
http://dx.doi.org/10.1002/jat.1385 PMID: 18756589

[37] Nel, A.; Xia, T.; Mädler, L.; Li, N. Toxic potential of materials at the nanolevel. *Science,* **2006**, *311*(5761), 622-627.
http://dx.doi.org/10.1126/science.1114397 PMID: 16456071

[38] Valko, M.; Izakovic, M.; Mazur, M.; Rhodes, C.J.; Telser, J. Role of oxygen radicals in DNA damage and cancer incidence. *Mol. Cell Biochem.,* **2004**, *266*, 37-56.
http://dx.doi.org/10.1023/B:MCBI.0000049134.69131.89

[39] Taner, G.; Aydın, S.; Bacanlı, M.; Sarıgöl, Z.; Şahin, T.; Başaran, A.A.; Başaran, N. Modulating effects of pycnogenol® on oxidative stress and DNA damage induced by sepsis in rats. *Phytother. Res.,* **2014**, *28*(11), 1692-1700.
http://dx.doi.org/10.1002/ptr.5184 PMID: 24919414

[40] Kim, H.Y.; Kim, J.K.; Choi, J.H.; Jung, J.Y.; Oh, W.Y.; Kim, D.C.; Lee, H.S.; Kim, Y.S.; Kang, S.S.; Lee, S.H.; Lee, S.M. Hepatoprotective effect of pinoresinol on carbon tetrachloride-induced hepatic damage in mice. *J. Pharmacol. Sci.,* **2010**, *112*(1), 105-112.
http://dx.doi.org/10.1254/jphs.09234FP PMID: 20093790

[41] Canesi, L.; Ciacci, C.; Fabbri, R.; Marcomini, A.; Pojana, G.; Gallo, G. Bivalve molluscs as a unique target group for nanoparticle toxicity. *Mar. Environ. Res.,* **2012**, *76*, 16-21.
http://dx.doi.org/10.1016/j.marenvres.2011.06.005 PMID: 21767873

[42] Wright, B.; Lacchini, A.H.; Davies, A.J.; Walker, A.J. Regulation of nitric oxide production in snail (*Lymnaea stagnalis*) defence cells: A role for PKC and ERK signalling pathways. *Biol. Cell,* **2006**, *98*(5), 265-278.
http://dx.doi.org/10.1042/BC20050066 PMID: 16293103

[43] Tafalla, C.; Novoa, B.; Figueras, A. Production of nitric oxide by mussel (*Mytilus galloprovincialis*) hemocytes and effect of exogenous nitric oxide on phagocytic functions. *Comp. Biochem. Physiol. B Biochem. Mol. Biol.,* **2002**, *132*(2), 423-431.
http://dx.doi.org/10.1016/S1096-4959(02)00050-7 PMID: 12031469

[44] Özel, R.E.; Alkasir, R.S.J.; Ray, K.; Wallace, K.N.; Andreescu, S. Comparative evaluation of intestinal nitric oxide in embryonic zebrafish exposed to metal oxide nanoparticles. *Small,* **2013**, *9*(24), 4250-4261. http://dx.doi.org/10.1002/smll.201301087 PMID: 23873807

[45] Hiraishi, H.; Terano, A.; Ota, S.; Mutoh, H.; Sugimoto, T.; Harada, T.; Razandi, M.; Ivey, K.J. Protection of cultured rat gastric cells against oxidant-induced damage by exogenous glutathione. *Gastroenterology,* **1994**, *106*(5), 1199-1207. http://dx.doi.org/10.1016/0016-5085(94)90010-8 PMID: 7909779

[46] Verma, R.S.; Mehta, A.; Srivastava, N. *In vivo* chlorpyrifos induced oxidative stress: Attenuation by antioxidant vitamins. *Pestic. Biochem. Physiol.,* **2007**, *88*(2), 191-196. http://dx.doi.org/10.1016/j.pestbp.2006.11.002

[47] Regoli, F.; Principato, G. Glutathione, glutathione-dependent and antioxidant enzymes in mussel, *Mytilus galloprovincialis*, exposed to metals under field and laboratory conditions: Implications for the use of biochemical biomarkers. *Aquat. Toxicol.,* **1995**, *31*(2), 143-164. http://dx.doi.org/10.1016/0166-445X(94)00064-W

[48] Madany, N.M.K.; Shehata, M.R.; Mohamed, A.S. Ovothiol-A isolated from sea urchin eggs suppress oxidative stress, inflammation, and dyslipidemia resulted in restoration of liver activity in cholestatic rats. *Biointerface Res. Appl. Chem.,* **2021**, *12*(6), 8152-8162. http://dx.doi.org/10.33263/BRIAC126.81528162

[49] Chelikani, P.; Fita, I.; Loewen, P.C. Diversity of structures and properties among catalases. *Cell. Mol. Life Sci.,* **2004**, *61*(2), 192-208. http://dx.doi.org/10.1007/s00018-003-3206-5 PMID: 14745498

[50] Livingstone, D.R. Organic Xenobiotic metabolism in marine invertebrates. *Adv. Comp. Environ. Physiol.,* **1991**, *7*, 45-185. http://dx.doi.org/10.1007/978-3-642-75897-3_2

[51] Hao, L.; Chen, L. Oxidative stress responses in different organs of carp (*Cyprinus carpio*) with exposure to ZnO nanoparticles. *Ecotoxicol. Environ. Saf.,* **2012**, *80*, 103-110. http://dx.doi.org/10.1016/j.ecoenv.2012.02.017 PMID: 22425733

[52] Yoloğlu, E.; Uçkun, M.; Uçkun, A.A. Metal accumulation and biochemical variations in the freshwater mussels (*Unio mancus*) collected from Atatürk Dam Lake, Turkey. *Biochem. Syst. Ecol.,* **2018**, *79*, 60-68. http://dx.doi.org/10.1016/j.bse.2018.05.006

[53] Jing, W.; Lang, L.; Lin, Z.; Liu, N.; Wang, L. Cadmium bioaccumulation and elimination in tissues of the freshwater mussel Anodonta woodiana. *Chemosphere,* **2019**, *219*, 321-327. http://dx.doi.org/10.1016/j.chemosphere.2018.12.033 PMID: 30551097

[54] Chandrasekaran, T.S.; Milton, J.; Santhanabharathi, B.; Pradhoshini, K.P.; Cojandaraj, L.; Priyadharshini, M.; Ahmed, M.S.; Musthafa, M.S.; Balaji, P.; Faggio, C. Heavy metals toxicity in edible bivalves and risk exposure to humans through its consumption from Adyar Estuary, Tamilnadu, India – A baseline study. *Reg. Stud. Mar. Sci.,* **2024**, *79*, 103854. http://dx.doi.org/10.1016/j.rsma.2024.103854